Medium Effects in Reactions with Rare Isotopes

C.A. Bertulani(1) **and M. Karakoç**(1,2)

(1) Department of Physics and Astronomy, Texas A&M University-Commerce, Commerce, TX 75429, USA

(2) Department of Physics, Akdeniz University, 07058, Antalya, Turkey

E-mail: `carlos_bertulani@tamu-commerce.edu`, `mesut_karakoc@tamu-commerce.edu`

Abstract. We discuss medium effects in knockout reactions with rare isotopes at intermediate energies. We show that the poorly known corrections may lead to sizable modifications of knockout cross sections and momentum distributions.

1. Introduction

Most practical studies of medium corrections in nucleon-nucleon scattering are carried out by considering the effective two-nucleon interaction in infinite nuclear matter. This is known as the G-matrix method, an is obtained from a solution of the Bethe-Goldstone equation

$$\langle \mathbf{k}|\mathrm{G}(\mathbf{P},\rho_1,\rho_2)|\mathbf{k}_0\rangle = \langle \mathbf{k}|\mathrm{v}_{NN}|\mathbf{k}_0\rangle - \int \frac{d^3k'}{(2\pi)^3}\frac{\langle \mathbf{k}|\mathrm{v}_{NN}|\mathbf{k}'\rangle Q(\mathbf{k}',\mathbf{P},\rho_1,\rho_2)\langle \mathbf{k}'|\mathrm{G}(\mathbf{P},\rho_1,\rho_2)|\mathbf{k}_0\rangle}{E(\mathbf{P},\mathbf{k}')-E_0-i\epsilon}, \tag{1}$$

with $\mathbf{k}_0$, $\mathbf{k}$, and $\mathbf{k}'$ the initial, final, and intermediate relative momenta of the NN pair, $\mathbf{k} = (\mathbf{k}_1 - \mathbf{k}_2)/2$ and $\mathbf{P} = (\mathbf{k}_1 + \mathbf{k}_2)/2$. If energy and momentum is conserved in the binary collision, $\mathbf{P}$ is conserved in magnitude and direction, and the magnitude of $\mathbf{k}$ is also conserved. v_{NN} is the nucleon-nucleon potential. E is the energy of the two-nucleon system, and E_0 is the same quantity on-shell. Thus $E(\mathbf{P},\mathbf{k}) = e(\mathbf{P}+\mathbf{k}) + e(\mathbf{P}-\mathbf{k})$, with e the single-particle energy in nuclear matter. It is also implicit in Eq. 1 that the final momenta $\mathbf{k}$ of the NN-pair also lie outside the range of occupied states.

In Ref. [1] the numerical calculations have been performed to account for the geometric effect of Pauli blocking. A parametrization has been devised which fits the numerical results. The parametrization reads

$$\begin{aligned}\sigma_{NN}(E,\rho_1,\rho_2) &= \sigma_{NN}^{free}(E)\frac{1}{1+1.892\left(\frac{2\rho_<}{\rho_0}\right)\left(\frac{|\rho_1-\rho_2|}{\tilde{\rho}\rho_0}\right)^{2.75}} \\ &\times \begin{cases} 1-\frac{37.02\tilde{\rho}^{2/3}}{E}, & \text{if} \quad E>46.27\tilde{\rho}^{2/3} \\ \frac{E}{231.38\tilde{\rho}^{2/3}}, & \text{if} \quad E\le 46.27\tilde{\rho}^{2/3}\end{cases}\end{aligned} \tag{2}$$

where E is the laboratory energy in MeV, ρ_i is the local density of nucleus i, $\rho_< = \min(\rho_1,\rho_2)$ and $\tilde{\rho} = (\rho_1+\rho_2)/\rho_0$, with $\rho_0 = 0.17$ fm^{-3}.

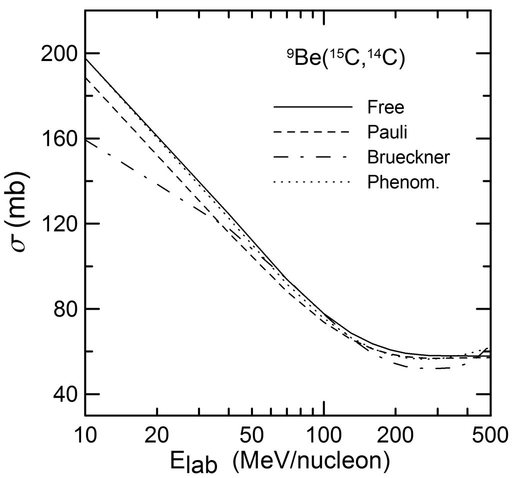

Figure 1. Total knockout cross sections for removing the $l = 0$ halo neutron of ^{15}C, bound by 1.218 MeV, in the reaction ^{9}Be(^{15}C,^{14}C$_{gs}$). The solid curve is obtained with the use of free nucleon-nucleon cross sections. The dashed curve includes the geometrical effects of Pauli blocking. The dashed-dotted curve is the result using the Brueckner theory, and the dotted curve is a phenomenological parametrization.

The Brueckner method goes beyond a treatment of Pauli blocking, and has been presented in several works, e.g. in Ref. [2, 3], where a simple parametrization was given, which we will from now on refer as Brueckner theory. It reads (the misprinted factor 0.0256 in Ref. [3] has been corrected to 0.00256)

$$\begin{aligned} \sigma_{np} &= \left[31.5 + 0.092 \left|20.2 - E^{0.53}\right|^{2.9}\right] \frac{1 + 0.0034E^{1.51}\rho^2}{1 + 21.55\rho^{1.34}} \\ \sigma_{pp} &= \left[23.5 + 0.00256 \left(18.2 - E^{0.5}\right)^{4.0}\right] \frac{1 + 0.1667E^{1.05}\rho^3}{1 + 9.704\rho^{1.2}} \end{aligned} \quad (3)$$

A modification of the above parametrization was done in Ref. [4], which consisted in combining the free nucleon nucleon cross sections parametrized in Ref. [5] with the Brueckner theory results of Ref. [2, 3]. Their parametrization, which better reproduce the nucleus-nucleus reactions cross sections, is

$$\begin{aligned} \sigma_{np} &= \left[-70.67 - 18.18\beta^{-1} + 25.26\beta^{-2} + 113.85\beta\right] \\ &\quad \times \tfrac{1+20.88E^{0.04}\rho^{2.02}}{1+35.86\rho^{1.9}} \\ \sigma_{pp} &= \left[13.73 - 15.04\beta^{-1} + 8.76\beta^{-2} + 68.67\beta^4\right] \\ &\quad \times \tfrac{1+7.772E^{0.06}\rho^{1.48}}{1+18.01\rho^{1.46}}, \end{aligned} \quad (4)$$

where $\beta = \sqrt{1 - 1/\gamma^2}$ and $\gamma = E[\mathrm{MeV}]/931.5+1$. We will denote Eq. 4 as the phenomenological parametrization.

We have performed a study of medium effects in knockout reactions which include different methods to treat medium effects [1]. To test the influence of the medium effects in nucleon knockout reactions, we consider the removal of the $l = 0$ halo neutron of ^{15}C, bound by 1.218 MeV, and the $l = 0$ neutron knockout from ^{34}Ar, bound by 17.06 MeV. The reaction studied is ^{9}Be(^{15}C,^{14}C$_{gs}$). The total cross sections as a function of the bombarding energy are shown in figure 1. The solid curve is obtained with the use of free nucleon-nucleon cross sections. The dashed curve includes the geometrical effects of Pauli blocking. The dashed-dotted curve is the result using the Brueckner theory, and the dotted curve is the phenomenological parametrization of the free cross section.

In figure 2 we plot the longitudinal momentum distributions for the reaction ^{9}Be(^{11}Be,^{10}Be), at 250 MeV/nucleon [1]. The dashed curve is the cross section calculated using the NN cross section from the Brueckner theory and the solid curve is obtained the free cross section. One

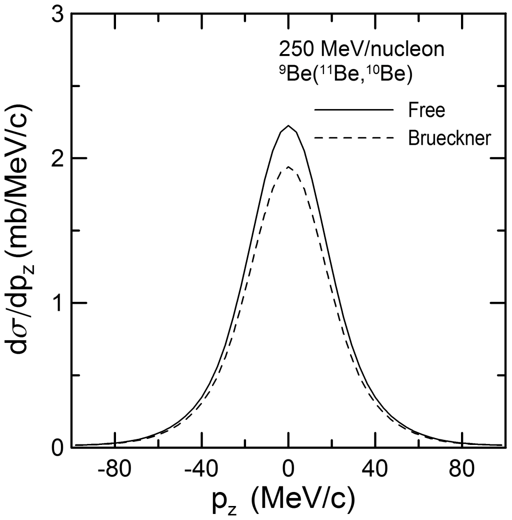

Figure 2. Longitudinal momentum distribution for the residue in the ^{9}Be(^{11}Be,^{10}Be), reaction at 250 MeV/nucleon. The dashed curve is the cross section calculated using the NN cross section from the Brueckner theory and the solid curve is obtained the free cross section.

sees that the momentum distributions are reduced by 10%, about the same as the total cross sections, but the shape remains basically unaltered. If one rescales the dashed curve to match the solid one, the differences in the width are not visible.

Based on these results we have developed a new version of the code MOMDIS [6] in order to treat medium effects an Coulomb recoil properly. A single nucleon removal cross section σ from the $J^{\pi} = 0^{+}$ the ground state (g.s.) of projectile to the g.s. of the knockout residue is given by

$$\sigma = \left(\frac{A}{A-1}\right)^{n} C^{2}S\sigma_{MOMDIS} \tag{5}$$

where σ_{MOMDIS} is calculated using a modified version of the MOMDIS code [6]. The A-dependent term is a center-of-mass correction to the shell-model spectroscopic factors ($C^{2}S$) where n is major oscillator shell number ($n = 1$ for sp shell nucleus ^{14}O and $n = 2$ for sd shell nucleus ^{36}Ca) [7, 8].

2. Proton and neutron knockout from rare isotopes

The reactions ^{9}Be(^{14}O,^{13}O), ^{9}Be(^{14}O,^{13}N) at 50 and 300 AMeV, and ^{9}Be(^{36}Ca,^{35}Ca), ^{9}Be(^{36}Ca,^{35}K) at 70.5 and 300 AMeV have been analyzed. The ground state spins for the nuclei ^{13}O, ^{13}N, ^{35}Ca and ^{35}K are respectively $3/2^{-}$, $1/2^{-}$, $1/2^{+}$ and $3/2^{+}$ and have been taken from Ref. [9], except for ^{35}Ca. The ground state spin for ^{35}Ca is not defined. We have assumed in our calculations it has $J^{\pi} = 1/2^{+}$ ground state spin.

The spectroscopic factors used in the present work are calculated with the shell model code NuShell@MSU [10], $C^{2}S$ considering the WBT interaction for ^{14}O [11] and USDA interaction for ^{36}Ca [12]. Our calculation is in agreement with Ref. [7] for ^{14}O proton removal case, but the neutron removal spectroscopic factor $C^{2}S$ for the present calculation is 34% bigger than in Ref. [7]. The bound state wave functions are calculated with Woods-Saxon potentials. We find that the ^{14}O proton removal result is in agreement with data from Ref. [7], but for neutron removal case there is a huge difference, probably due to the very big value of $C^{2}S = 4.97$.

Recently, the ^{12}C(^{23}Al,^{22}Mg)X knockout reaction has been measured at 50 MeV/nucleon to investigate the ground state properties of ^{23}Al [13]. A. Banu *et al.* showed that the ground-state structure of ^{23}Al is a possible configuration mixing of a d-orbital valence proton coupled to four core states of ^{22}Mg - 0^{+}_{gs}, 2^{+}_{1}, 4^{+}_{1}, 4^{+}_{2}. They also confirmed the ground state spin and parity of ^{23}Al as $J^{\pi} = 5/2^{+}$ and obtained the asymptotic normalization coefficient of the nuclear system

$^{23}\mathrm{Al}_{gs} \rightarrow {}^{22}\mathrm{Mg}(0^+) + \mathrm{p}$ as $C^2_{d_{5/2}}(^{23}Al_{gs}) = (3.90 \pm 0.44) \times 10^3\ \mathrm{fm}^{-1}$. Their results are shown in Fig. 3.

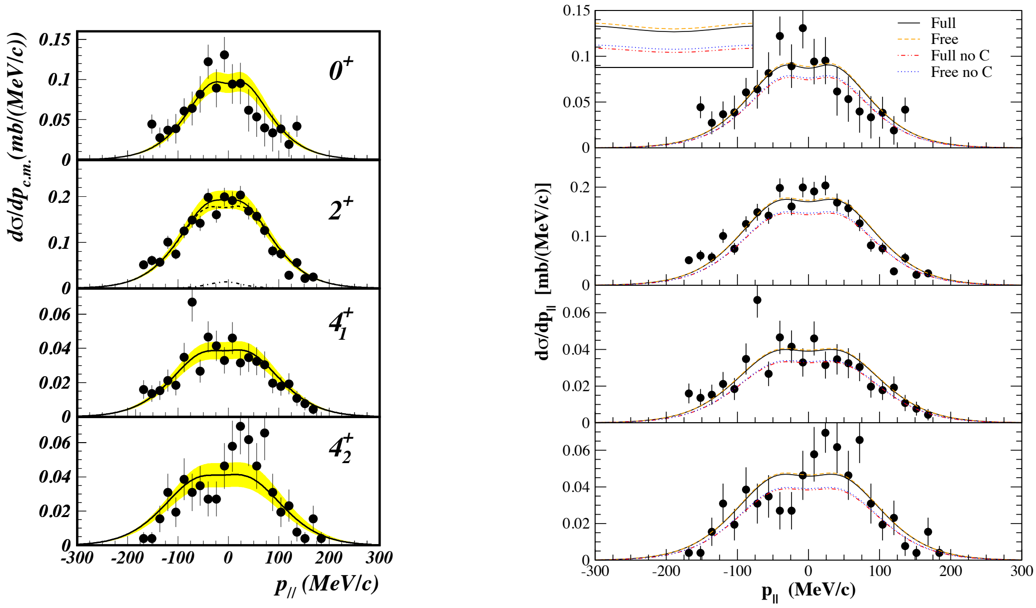

Figure 3. Left: Exclusive longitudinal momentum distributions. Shaded areas correspond to 1σ deviation in the spectroscopic amplitudes [13]. Right: Same data compared with our calculations. "Full" has both Coulomb and medium corrections. "Free" has no medium corrections. "no C" means calculations without Coulomb corrections.

In figure 3 we show the exclusive longitudinal momentum distributions extracted from Ref. [13]. Shaded areas correspond to 1σ deviation in the spectroscopic amplitudes [13]. On the right panel we compare the data compared with our calculations. "Full" has both Coulomb and medium corrections. "Free" has no medium corrections. "no C" means calculations without Coulomb corrections. We see that the medium and Coulomb final state interactions yield a spread on the results comparable to the uncertainty arising from 1σ deviations in the spectroscopic amplitudes. It is therefore clear that medium corrections and final state interactions are of extreme relevance for extracting spectroscopic information from knockout reactions. Work in this direction is in progress [14].

References

[1] C.A. Bertulani and C. De Conti, Phys. Rev. C 81, 064603 (2010).
[2] G. Q. Li and R. Machleidt, Phys. Rev. C 48, 1702 (1993).
[3] G. Q. Li and R. Machleidt, Phys. Rev. C 49, 566 (1994).
[4] Cai Xiangzhou, et al, Phys. Rev. C58, 572 (1998).
[5] S. K. Charagi and S. K. Gupta, Phys. Rev. C 41, 1610 (1990).
[6] C. Bertulani and A. Gade, Comp. Phys. Comm. 175, 372 (2006).
[7] C. Louchart, A. Obertelli, A. Boudard, and F. Flavigny, Phys. Rev. C 83, 011601 (2011).
[8] A. Gade et al, Phys. Rev. C 77, 044306 (2008).
[9] National Nuclear Data Center (nndc), Brookhaven National Laboratory, available at http://www.nndc.bnl.gov/nudat2/.
[10] B. A. Brown and W. Rae (2007), private communication.
[11] E. K. Warburton and B. A. Brown, Phys. Rev. C 46, 923 (1992).
[12] B. A. Brown and B. H. Wildenthal, Annu. Rev. Nucl. Part. Sci. 38, 29 (1988).
[13] A. Banu, et al, Phys. Rev. C 84, 015803 (Jul. 2011).
[14] M. Karakoç and C.A. Bertulani, in preparation.